Assessment of Active Tectonics of Giri Valley, NW Himalaya: Insights from Geomorphic Signature Using Remote Sensing and GIS

Raghuveer Negi*[1], Saraswati P. Sati[2], Mohit K. Puniya[3], Mery Biswas[4]
Tripti Jayal[5], Ashish Rawat[6], Sanjay S. Rana[1], Vikram Sharma[7]

Abstract

The landforms in the tectonically active region are regulated and modified by both external (climatic) and internal dynamic (tectonic) processes. The imprints of active deformation are stored in the form of geomorphic features such as fossils valley, sag ponds, narrow and wide valleys, pools and rapids, etc. We studied 12 geomorphic indices that have a direct relationship with tectonics using an SRTM-30m (1-arc second) spatial resolution Digital Elevation Model (DEM) coupled with Geographic Information System (GIS) tools. For detailed analysis, we have selected 19 sub-watershed (SW) of the Giri river basin. The geomorphic signatures of active tectonics are quantified in the present study to assess the active tectonics in the Giri valley. The current study suggests 15 SW are highly active and the remaining 4 SW are comparatively less active.

Keywords: *Active Tectonics, Geomorphology, Longitudinal Profile, Giriwatershed, SL and SI Index*

[*1] **Raghuveer Negi, Sanjay S. Rana,** Department of Geology, DBS PG College Dehradun, Uttarakhand, 248001, India.
[2] **Saraswati P. Sati,** Department of Basic and Social Sciences, College of Forestry, Ranichouri, Tehri Garhwal, Garhwal U.K. (VCSGUUHF Bharsar, Pauri Garhwal), Uttarakhand, 249199, India.
[3] **Mohit K. Puniya,** Department of Research and Innovation, Uttaranchal University Dehradun, 248001, India
[4] **Mery Biswas,** Department of Geography, Presidency University, 86/1, College Street, Kolkata 700073, West Bengal, India.
[5] **Tripti Jayal,** State environment conservation and climate change directorate, Dehradun, Uttarakhand, 248001, India.
[6] **Ashish Rawat,** Department of Geology, School of Earth Sciences, HNB Garhwal University Srinagar Garhwal, Uttarakhand, 249161, India.
[7] **Vikram Sharma,** Department of Geography, Institute of Sciences, Banaras Hindu University, Banaras, Uttar Pradesh, 221005, India.
[*] Corresponding Author Email: raghuveer750@gmail.com, https://orcid.org/0000-0002-7000-2808, Mob.: +919897835558

1. Introduction

The collision of the Indian and Eurasian plates has initiated Himalaya orogeny. The continuous plate movement has shaped the present-day Himalayas. As a consequence of continuous tectonic plate interaction, the Himalayan Mountains are tectonically active and steadily rising (Dewey and Bird, 1970; Burey and Dewey, 1973; DeMets et al., 1994; Singh et al., 2002; Yin, 2006; Puniya et al., 2019). The convergence rate may vary from place to place along the Himalayan mountain belt (Jayangondaperumal et al., 2020). Nakata (1972) was the first to study active tectonics in the Himalayas along the Sub-Himalaya foothill in Pinjor, Dehradun, and Bengal (Jayangondaperumal et al., 2020). The Global Positioning System (GPS) observation suggested a convergence rate of 18±1 mm/ year in the N213°E (Yadav et al., 2019; Gautam et al., 2017; Jayangondaperumal et al., 2020). Tectonics plays a crucial role in the deformation of rocks and landforms in the tectonically active terrain. The deformation leads to the fragile and weak nature of rocks resulting in a higher rate of denudation which eventually changes the topography and accelerates the landslide activities in the Himalayas (Kumar et al., 2017; Sah et al., 2018; Thakur et al., 2023). The geomorphic agents like rivers and glaciers are primary sources of denudation processes in the region (Kumar et al., 2017; Sah et al., 2018; Negi et al., 2021). The landform developed as a result of tectonics can be quantified to assess the active tectonics prevalent in the region.

Geological and geomorphological tools have constantly been used to assess the sensitivity and expressions of active tectonics in the Himalayan Mountain region in the past (Yin, 2006; Webb et al., 2007; Sati et al., 2008; Webb et al., 2011; Jain et al., 2016; Lone, 2017; Jayangondaperumal et al., 2020; Kothyari et al., 2019, 2022). The geomorphic indices are used in the present study as they are widely used to understand the development of geomorphic landforms and to delineate the tectonically active region in mountainous terrain (Keller and Pinter, 1996; Mesa, 2006; Pérez-Peña et al., 2009; Ozdemir and Bird, 2009; Sharma et al., 2018; Vijith et al., 2018). The geomorphic study includes a quantitative assessment of the watersheds (Strahler, 1964). The geomorphic indices used in the present study are effective tools in assessing the changes in landform owing to folding and faulting of litho-tectonic unit. Geomorphic indicators of tectonic activity in such terrain includes varying river course or drainage network set-up, variability in valley incision, basin asymmetry, basin tilt, basin shape,

etc. (Cox, 1994; Sharma et al., 2018; Rawat et al., 2021; Biswas et al., 2021; Dasgupta et al., 2022). In the present work, an approach using a combination of tools viz. topographic map, aerial photograph, and satellite data in a Geographic information system (GIS) platform is done to decipher the active tectonics in the Giri river Watershed (Kothyari and Juyal 2013; Kothyari et al., 2017; Biswas and Paul, 2021; Biswas et al., 2021; Dasgupta et al., 2022). The salient objective of the present work is to assess the tectonic activities in GW and examine the role of local or regional tectonics in shaping the present-day landforms.

2. Geological Setup

The Giri Watershed (GW) lies between latitude 30° 26' 29" N to 31° 15' 9" N and longitude 77° 0' 0" E to 77° 50' 55 "E (Fig 1) covering approximately an area of 2628 km². The Giri River originates from the Kupper of Simla district and flows through three districts

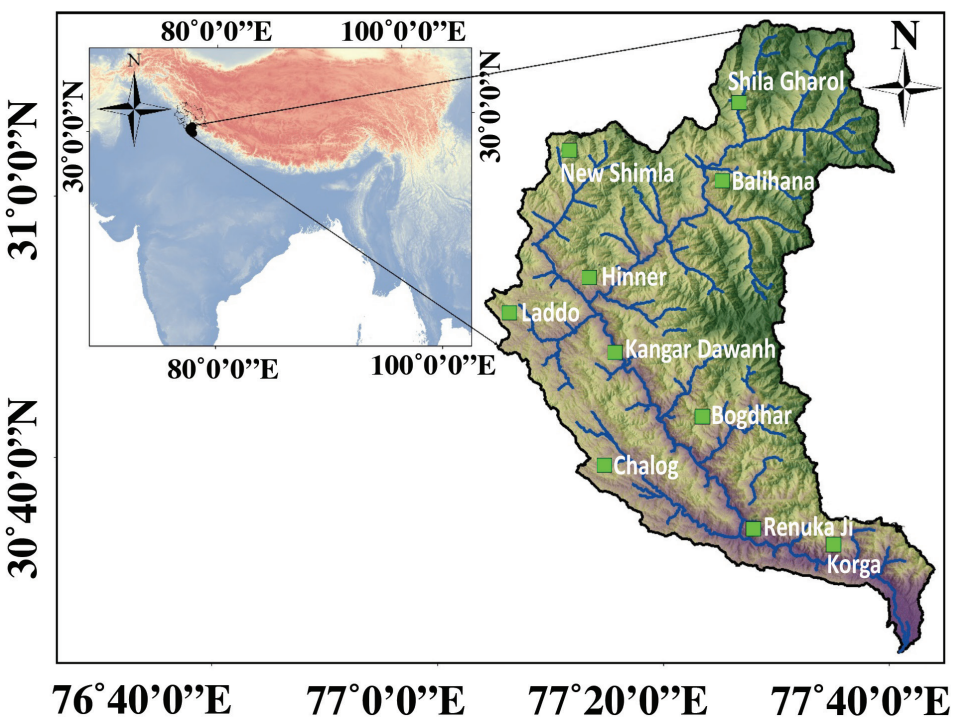

Figure 1 : Location for the Giri Watershed, Himachal Pradesh, Northwest Himalaya, India.

viz. Solan, Simla, and Sirmour, before joining the Yamuna River near Paonta Sahib. The major tributaries of Giri River are Jalal, Assani, Kwali, Ghamber, Satana, Pervi, Chakhred, Bhajetu, Baseri, etc. The altitude in GW varies from 395 m to 3623 m while mean elevation is 1686 m above mean sea level.

Geologically GW constitutes the part of Northwest Himalaya and is composed of Quaternary alluvium, Cenozoic Sedimentary rocks sequence of Sub-Himalaya Sedimentary (SHS) and Meta Sedimentary rocks sequence of Lesser Himalaya (LHS), and Metamorphic and crystalline rocks rock of the Higher Himalaya (HHS) (Fig 2a). The SHS comprises Siwalik and Sirmour Group (Srikantia and Bhargava, 1998; Biyani, 2007; Mishra and Mukhopadhyay, 2012; Srikantia and Bhargava, 2021). The Siwalik group in GW is composed of the Lower Siwalik (Kamlial Formation) rocks that are delimited in the north by the Main Boundary Fault (MBT). Sirmour group is divided into Subathu, Dagashai, and Kasauli formations (Srikantia and Bhargava, 1998; Mishra and Mukhopadhyay, 2012; Srikantia and Bhargava, 2021) (Fig 2a).

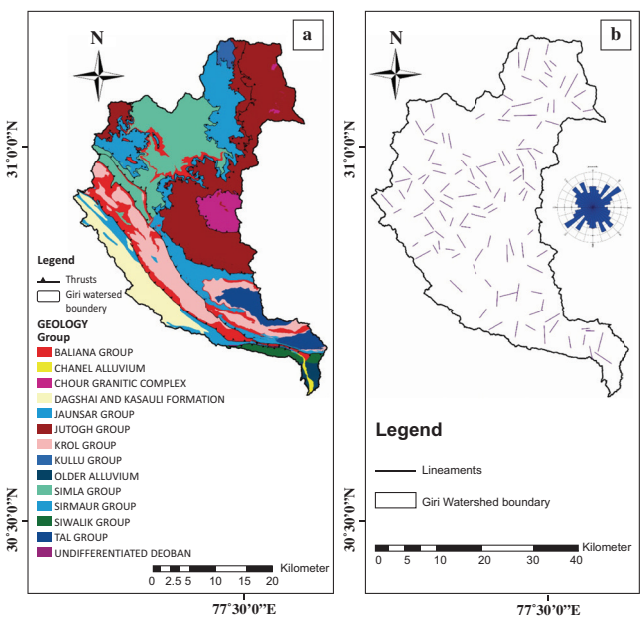

Figure 2 : Fig showing (a) Geological Map (Mukhopadhyay et al., 1996; GSI, 2019) and Major (b) Lineament for the Giri Watershed, NW Himalaya, India.

The LHS includes the rocks of the Deoban group, Jaunsar group (Nagthat, Mandhali, and Chandpur formations), Simla group (Sanjauli, Chhoasa, and Basanatpur Formations), Baliana group (Blaini, and Infrakrol Formations), Krol Group (Kauriyala, Jarassi, Mahi and Chambaghat Formations), and Tal group (Kotidhiman, Sankholi, and Shaliyan Formations) that are delimited by the Jutogh thrust and MBT in North and South respectively (Fig 2a). The old Proterozoic rocks of the Simla and Jaunsar group are separated from the younger rocks of Cenozoic (Sirmour group) by two folded thrust planes (i.e. Krol Thrust and Giri thrust) that are possibly two traces of single thrust (Srikantia and Bharagava, 1998; Singh et al., 2020; Srikantia and Bhargava, 2021). The rocks of the Baliana group overlie the Simla group rocks uncomfortably in GW along with the Jaunsar thrust (Fig 2a) (Srikantia and Bharagava, 2021).

The Higher Himalaya sequence in GW includes the Rocks of the Kullu group (Kokhan Formation), Jutogh group (Naura, Kanda, Taradevi, Khirkhi, Bhotli, Manal, and Panjreli Formations), and Chaur Granitic Complex (Fig 2a). The Kokhan Formation rocks are separated by Jaunsar thrust and Kullu thrust in GW (Fig 2a). The Rocks of the Chaur Granitic Complex are separated by the Chaur thrust from the rocks of the Jutogh group. The rocks of The Bhotli formation and Khirki formation of the Jutogh group is separated by the Khirkhi thrust (Srikantia and Bhargava, 1998; Hughes et al., 2005; Jamwal and Wangu, 2012; Mishra and Mukhopadhyay, 2012; Bhargava and Srikantia, 2014; Dhital, 2015; Mukherjee, 2015; Singh et al., 2020; Srikantia and Bhargava, 2021).

3. Data And Methodology

Morphometric analysis of the GW has been evaluated using remote sensing data and GIS techniques. The Shuttle Radar Topographic Mission-Digital elevation model (SRTM-DEM) (downloaded from https://earthexplorer.usgs.gov) with a spatial resolution of 30 meters has been used for extractions of drainage and delineations of watershed boundary and sub-watersheds (SW) boundary (Fig 3). The drainage extracted from the SRTM DEM have been further referenced and rectified with Survey of India (SOI) toposheet (53E/4,7,8,11,12, and 53F/1,2,5,6,7,9,10,11) in 1:50,000 scale. The watershed and sub-watershed boundary have been delineated using the pour point method in the GIS. The Geological map (Fig 2a) of Geological Survey of India (GSI) in 1:50000 scale

(https://bhukosh.gsi.gov.in/Bhukosh/MapViewer.aspx) and Mukhopadhyay et al., (1996) has been modified and digitized in GIS platform. The lineaments are extracted and a lineaments map of the study area is prepared from Sentinel-2 and SRTM-DEM satellite data.

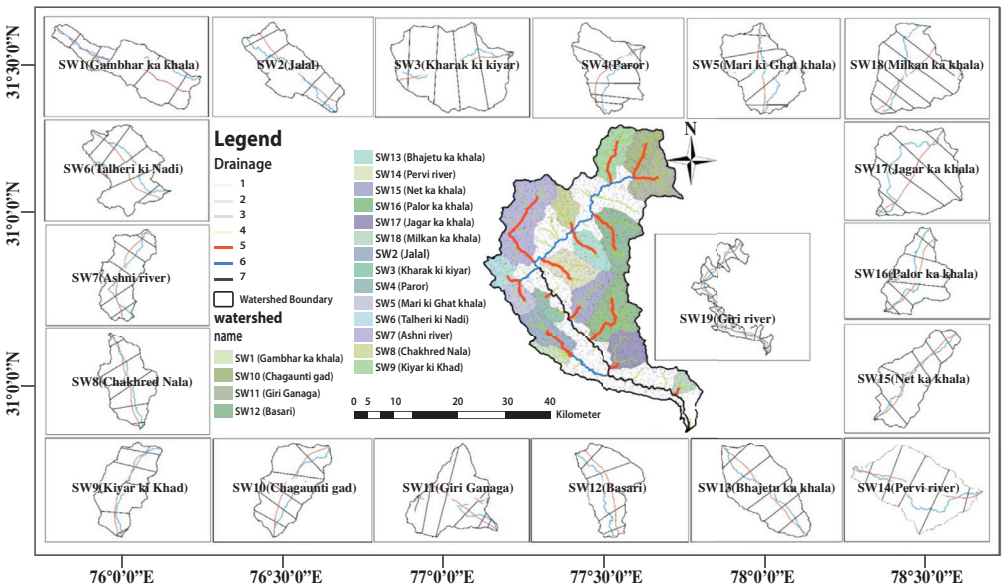

Figure 3 : Showing Drainage Map, Sub-Watershed Map, T and Vf Calculation Section Map for Giriwatershed, Himachal Pradesh, Northwest Himalaya, India.

The GW has been divided into 19 SW based on 5th order stream (except SW19 with 7th order basin) (Fig 3). The morphometric indices have been divided into two broad categories i.e. Spatial Aspects, and Linear Aspects. The Spatial aspects include parameters like *Drainage density (D_d), Circulatory ratio (R_c), Form factor (F_f), Basin shape index (B_s), Lemniscate Coefficients (K), Asymmetry factors (A_f), Transverse topographic symmetrical factor (T), Valley floor to width to the height ratio (Vf), Hypsometric Curve (HC), and Hypsometric Integral (HI), while Linear Aspects includes Sinuosity Index (S_I), Stream Length Gradient Index (S_L), Longitudinal river profile, and major Lineaments* (Table 1)

Table 1 : Formulae used for the Evaluation of Morpho-Tectonic Parameter of Giriwatershed Himachal Pradesh, Northwest Himalaya India.

Aspects	Parameter	Formula	Descriptions	References
Spatial Aspects	Drainage density (D_d)	$D_d = \frac{L\mu}{A}$	L_μ is total stream length, A is area of watershed.	Horton (1945)
	Circularity ratio (R_c)	$F_f = \frac{A}{Lb^2}$	A is the area of the watershed, Lb^2 is the square of the basin length.	Horton (1945)
	Ruggedness Number (R_n)	$R_c = \frac{4\pi A}{p^2}$	4 is constant, ϖ is constant i.e. 3.14, and P is the perimeter of the basin or watershed.	Miller (1953)
	Basin shape Index (B_s)	$R_n = R \times D_d$	R is the relief of the basin or watershed and D_d is the drainage density.	Ramırez-Herrera, 1998)
	Transverse topographic Symmetrical factor (T)	$B_s = \frac{L_b}{vfw}$	V_{fw} is the valley floor width and L_b is the length of the valley.	Cox (1994); Keller and Pinter (1996)
	Asymmetrical Factor (A_f)	$T = \frac{D_a}{D_d}$	Da is the distance of the drainage to the mid channel, and Dd is the distance of the stream from the drainage divide.	Hare and Gardner (1985); Keller and Pinter (1996)
	Valley floor width to the Height ratio (V_f)	$A_f = \frac{A_r}{A} \times 100$	A_r is the area in the right-side sides of the stream in the watershed, A total area of the watershed or basin.	Bull and McFadden (1977); Keller and Pinter (1996)
	Lemniscat's Cofficient (K)	$V_f = \frac{2vfw}{(H1-H3)+(H2-H3)}$	2 is the constant and V_{fw} is the valley floor width, H1 and H2 are left and right-side elevation of the valley divides respectively, and H3 is the elevation of the valley floor.	Chorley et al., 1957

Aspects	Parameter	Formula	Descriptions	References
	Lemniscat's Cofficient (K)	$K = \frac{Lb^2}{A}$	Lb^2 is the square of the basin length, and A is the total area of the basin or watershed.	
	Hypsometric Integral (HI)	$E \approx HI = \frac{Elev_{Mean} - Elev_{Min}}{Elev_{Max} - Elev_{Min}}$	Elevmean is the mean elevation, Elevmin and Elevmax is the lowest and highest elevations of the watershed or basin.	Pike and Wilson (1971)
Linear Aspects	Stream Length Gradient Index (SL)	$S_L = \frac{\wedge H}{\wedge L} \times L$	Where, ΔH is the elevation difference of the stream segment, ΔL length of the stream segment, and L is the horizontal length from the midpoint of the stream segment to the watershed divide.	Hack (1973)
	Sinuosity Index (SI)	$S_I = \frac{A_L}{S_L}$	AL is the actual stream length of main stream, SL is the straight stream length of the main stream	Mueller (1968); Haggett and Chorley (1969)

The parameter like S_I, S_L, V_f, and T have been calculated segment-wise (Fig 3). The segment of the river for S_I and S_L have been divided according to the natural break (Jenks) in GIS (Fig 4; 5, 6), while T and V_f have been calculated segment-wise for each SW. The value of spatial and linear aspects is divided into the four classes of active tectonics, where Class-1 (Very high), Class-2 (High), Class-3 (Moderate), and Class-4 (Low) respectively suggests comparative activeness of tectonics in SW. The coefficient of determination (R^2) for the longitudinal profile has been calculated using the following equation:

The linear function: $y=ax+b$. (1)

The exponential function: $y=ae^{bx}$. (2)

The logarithmic function: $y=alnx+b$. (3)

The power function: $y=ax^b$. (4)

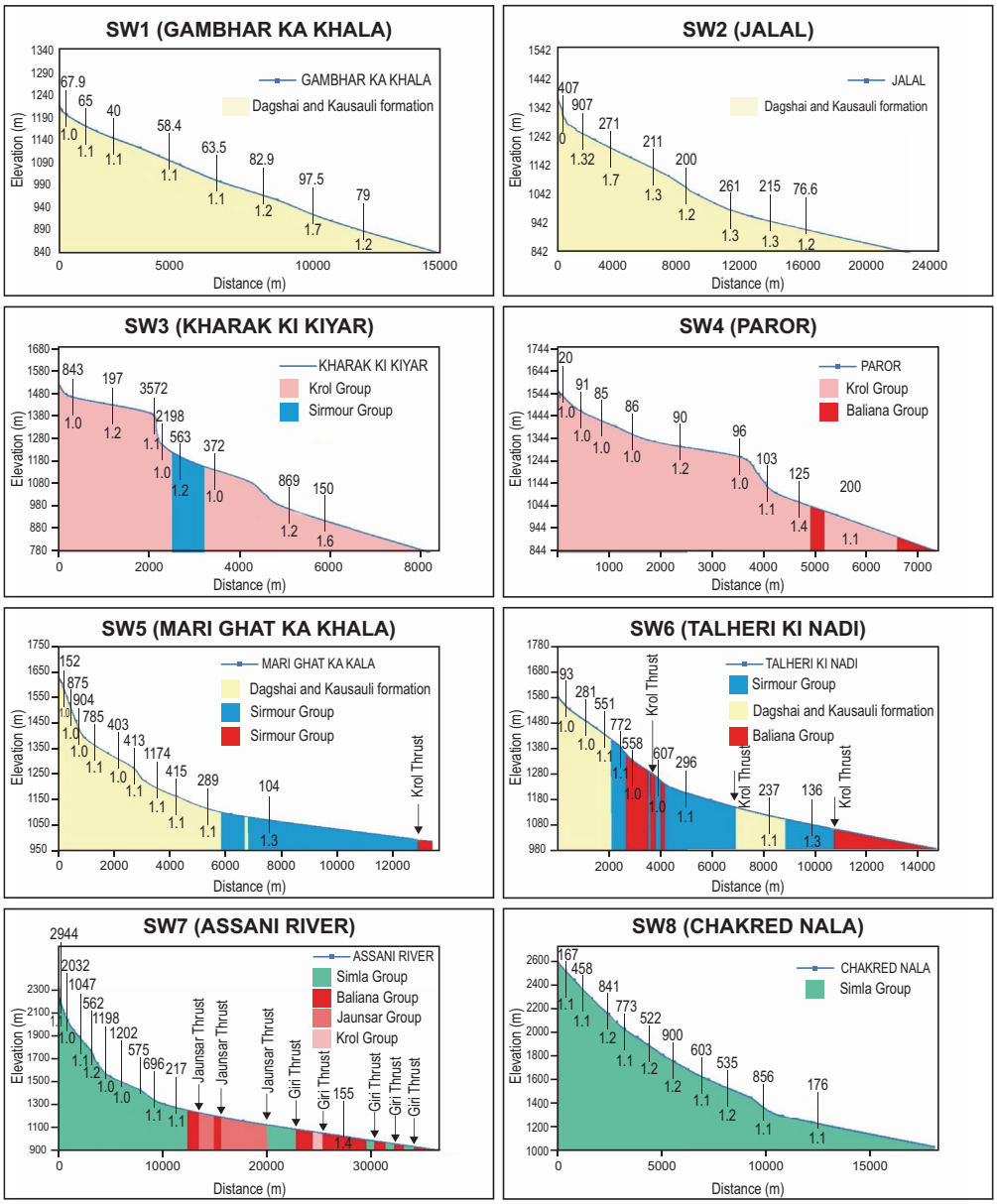

Figure 4 : Showing Examples of the Longitudinal Profile of the River SW1 to SW8. Numerical Value Inset in the Diagram above River SL and Below S_l

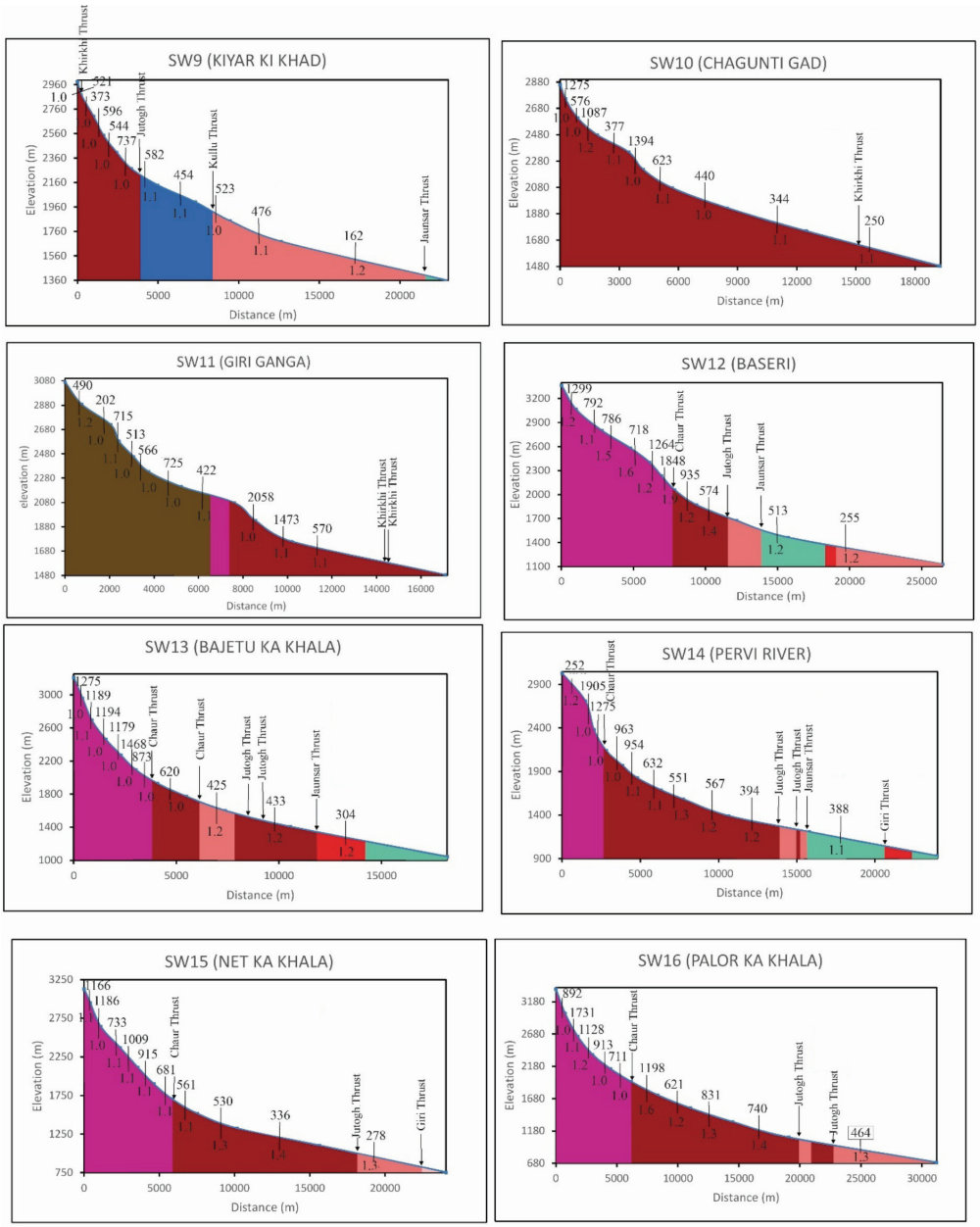

Figure 5 : Showing examples of the longitudinal profile of the River SW9 to SW16. Numerical value inset in the diagram above River SL and Below SI.

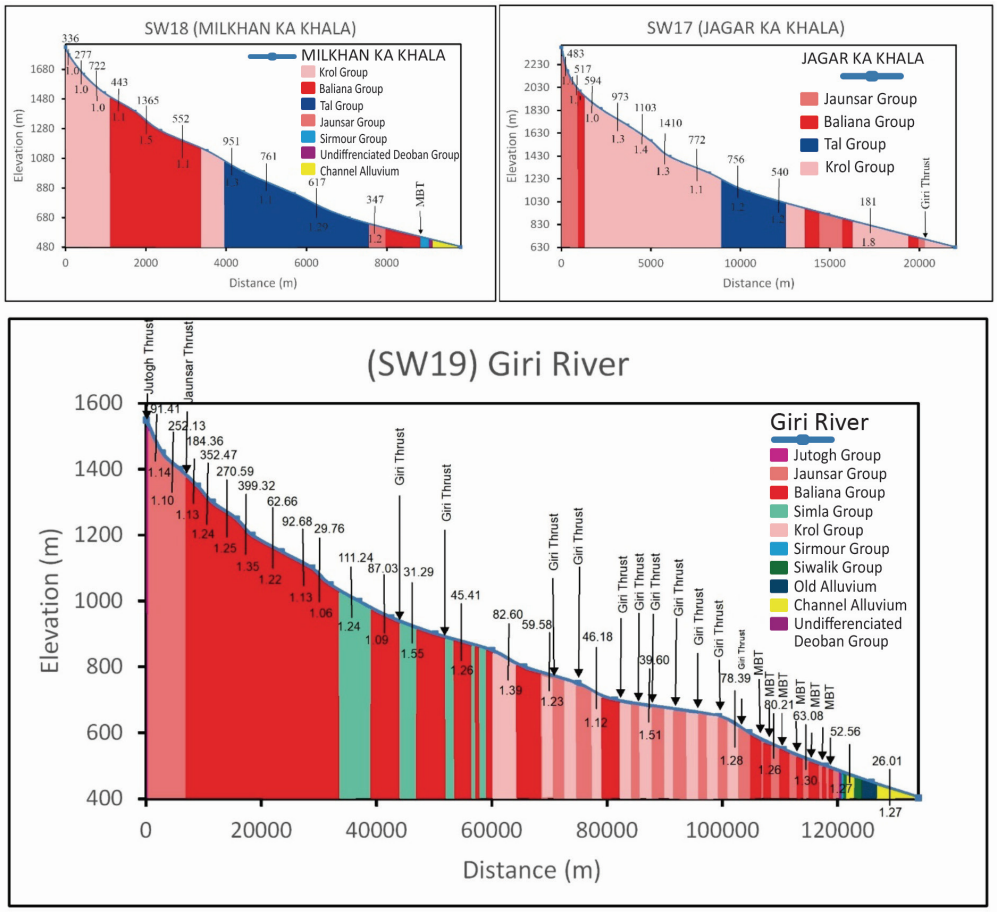

Figure 6 : Showing examples of the longitudinal profile of the River SW17 to SW19. Numerical value inset in the diagram above River SL and Below SI.

RESULTS

3.1. Spatial Aspects

3.1.1. Drainage Density (Dd)

The Dd is obtained as the ratio of Lμ of all stream networks to the area of the watershed,

which is an expression of stream in a unit area (Horton, 1945; Strahler, 1964). The D_d is an indicator of dissected and linear topography formed as a result of erosional and fluvial processes and D_d depends on the nature of the rocks, soil strength, and the relief of the area (Singh, 2002; Das and Gupta, 2019). In tectonically active terrains, the D_d signifies the intense deformation and fragile nature of rocks and its value increases with higher rate of deformation and uplift (Rawat et al., 2021). The value of D_d for 19 SW ranges from 2.17 to 2.66 (Table 2) in present study. Based on activeness of tectonics the value of Dd has been divided into Class-1 (> 2.54), Class-2 (2.42-2.53), Class-3 (2.30-2.41), and Class-4 (< 2.29) for the GW (Table 3).

Table 2 : Table Showing Morpho-Tectonic Parameter (where Al –Alluvium, Sw-Siwalik group, Sb-Subathu Formation, Dk- Dagshai and Kasauli Formation, De- Deoban Group, Ja- Jaunsar Group, Sm- Simla Group, Ch- Chaur Granitic Complex, Ju- Jutogh Group, Kl-Kullu Group, Ba-Baliana group, Kr- Krol Group, Tl- Tal Group)

Subwatershed	A_f	B_s	F_f	R_c	K	D_d	R_n	HI	T avg	V_f avg	Geology	Thrusts
SW1 (Gambhar ka khala)	65.54	4.09	0.13	0.37	7.63	2.23	1.56	0.49	0.39	0.14	Dk	
SW2 (Jalal)	41.67	3.00	0.18	0.45	5.62	2.41	2.90	0.47	0.38	0.18	Dk, Sb, Ba, Kr	KrT
SW3 (Kharak ki kiyar)	74.73	1.28	0.38	0.68	2.60	2.17	2.53	0.54	0.18	0.23	Sb, Kr	
SW4 (Paror)	37.70	1.05	0.40	0.54	2.47	2.26	2.69	0.51	0.23	0.33	Kr, Ba	
SW5 (Mari ki ghat khala)	39.75	1.92	0.30	0.62	3.29	2.45	2.17	0.48	0.24	0.14	Sb, Dk, Ba	KrT
SW6 (Talheri ki Nadi)	63.76	1.66	0.33	0.42	3.04	2.63	2.67	0.48	0.19	0.13	Sb, Dk, Ba, Kr	KrT
SW7 (Ashni river)	56.62	2.99	0.19	0.42	5.17	2.52	4.46	0.48	0.21	0.15	Ba, Kr, Ja, Ju, Sm,	GrT, JaT, JuT
SW8 (Chakhred Nala)	54.33	2.27	0.24	0.52	4.21	2.43	4.15	0.51	0.22	0.13	Sm, Ba, Ja	JaT

Subwatershed	A_f	B_s	F_f	R_c	K	D_d	R_n	HI	T avg	V_f avg	Geology	Thrusts
SW9 (Kiyar ki Khad)	57.96	2.48	0.23	0.54	4.39	2.40	4.39	0.50	0.20	0.07	Ja, Kl, Ju	JaT, KuT, JuT
SW10 (Chagaunti gad)	64.09	2.37	0.23	0.58	4.28	2.66	4.53	0.50	0.25	0.04	Ju	KhT
SW11 (Giri Ganaga)	55.00	0.96	0.65	0.53	1.53	2.39	4.11	0.49	0.40	0.12	Ju	KhT
SW12 (Basari)	68.99	2.14	0.23	0.51	4.39	2.35	5.87	0.46	0.34	0.16	Ju, Ch, Sm, Ja, Ba	ChT, JaT, JuT
SW13 (Bhajetu ka khala)	50.60	2.37	0.25	0.65	4.01	2.37	5.57	0.47	0.27	0.21	Ju, Ch, Sm, Ja, Ba	ChT, JaT, JuT
SW14 (Pervi river)	62.70	2.47	0.19	0.56	5.24	2.50	5.58	0.44	0.30	0.16	Ju, Ch, Sm, Ja, Ba	ChT, JaT, JuT,GrT
SW15 (Net ka khala)	47.47	2.95	0.18	0.47	5.63	2.48	6.52	0.46	0.19	0.19	Ch, Ju, Ja, Kr,	ChT, JuT, GrT
SW16 (Palor ka khala)	40.20	2.00	0.19	0.48	5.13	2.50	7.27	0.45	0.37	0.12	Ch, Ju, Ja, Kr, Ba	JuT, GrT
SW17 (Jagar ka khala)	32.93	1.83	0.21	0.64	4.72	2.23	4.00	0.50	0.34	0.10	Ja, Ba, Kr, Tl	GrT
SW18 (Milkan ka khala)	36.42	1.50	0.33	0.62	2.99	2.35	3.59	0.50	0.36	0.25	Kr, Ba, Tl, Ja, De, Sb	MBT
SW19 (Giri river)	54.57	6.03	0.05	0.07	21.95	2.50	6.48	0.43	0.38	0.87	Sw, Dk, Kr, Ba, Tl, Ja, De, Sb Ch, Ju, Sm, Tl, Al	MBT, JaT, JuT, GrT, KrT, KhT,

Table 3 : Active Tectonic Classification Based on Value of Geomorphic Indices for GW.

Aspects	Parameter	Active tectonics classes			
		Class I	Class II	Class III	Class IV
Spatial Aspects	Drainage density (D_d)	> 2.54	2.53 – 2.42	2.41 – 2.30	< 2.29
	Form factor (F_f)	< 0.20	0.21 – 0.35	0.36 – 0.50	> 0.51
	Circularity ratio (R_c)	< 0.44	0.45 – 0.52	0.53 – 0.60	> 0.61
	Ruggedness Number (R_n)	> 5.85	5.84 – 4.41	4.40 – 2.98	< 2.97
	Basin shape Index (B_s)	> 3.31	3.30 – 2.53	2.52 - 1.75	< 1.74
	Transverse topographic Symmetrical factor (T)	> 0.62	0.61 – 0.42	0.41 – 0.22	< 0.21
	Asymmetrical Factor (A_f)	> 68.1	68 – 60, and 31 - 37	37 – 42, and 57 - 60	45 - 60
	Valley floor width to the Height ratio (V_f)	< 0.24	0.25 – 0.45	0.46 – 0.66	> 0.67
	Lemniscat's Cofficient (K)	> 6.11	6.10 – 4.59	4.58 – 3.06	< 3.05
	Hypsometric Integral (HI)	> 0.51	0.50 – 0.48	0.47 – 0.45	< 0.44
Linear Aspects	Stream Length Gradient Index (S_L)	> 2689	2688 - 1797	1796 - 909	< 908
	Sinuosity Index (S_I)	> 1.64	1.63 – 1.43	1.42 – 1.22	< 1.21

3.1.2 Form Factor (F_f)

The Ff is a shape parameter and is the ratio of the area of the watershed to the square of the basin or watershed length (L_b) (Horton, 1945). The shape of the basin is influenced by active tectonics, as the regional structures like faults or thrust influence the surface processes in the watershed which shapes the topography of a watershed. The F_f value ranges between 0 (Elongated shape) to 1 (Circular shape) where the values close to 0 are associated with higher rate of tectonic activity and values close to 1 suggest weak influence of tectonic activity (Wołosiewicz, 2018). The F_f values for 19 SW range from

0.05 to 0.65 (Table 2) in GW. The Ff values obtained have been divided into the Class-1 (< 0.20), Class-2 (0.21 – 0.35), Class-3 (0.36 – 0.50), Class-4 (> 0.51) based on the influence of tectonic activity (Table 3).

3.1.3 Circularity Ratio (R_c)

The R_c is also a shape factor that determines the influence of tectonics on the development of shape of a watershed. The R_c value close to 1 is associated with a circular shape and low influence of lithology, regional or local structures; while values close to 0 indicates elongated shape and tectonically active terrain (Miller, 1953, Rawat et al., 2021). The values of R_c ranges between 0.07 to 0.68 (Table 2), which are divided accordingly into Class-1 (< 0.44), Class-2 (0.45 – 0.52), Class-3 (0.53 – 0.60), and Class-4 (> 0.61) based on tectonic behavior of the terrain (Table 3).

3.1.4 Basin Shape Index (Bs)

The B_s can be calculated as the ratio of basin length to the width (calculated at the widest point) within the watershed or basin (Ramírez-Herrera, 1998). The shape of the drainage basin or watershed is a significant indicator of tectonic control (Sharma et al., 2018). In addition to the contrast, the stable and senile drainage basins are characterized by the widening of the basin (Ramírez-Herrera, 1998; Mahmood and Gloaguen, 2012). The B_s value for 19 SW varies from 0.96 to 6.03 (Table 2). The values of B_s have been divided into Class-4 (< 1.74), Class-3 (1.75 – 2.52), Class-2 (2.53 – 3.30), and Class-1 (> 3.31) based on the influence of tectonics (Table 3).

3.1.5 Lemniscate Coefficients (K)

The K is used as a measurement of the gradient of the Basin or watershed (Chorley et al., 1957). The *K* value ranges from 1.53 to 21.95 (Table 2) for 19 SW in GW. The higher values of *K* indicate a higher rate of tectonic activity in the basin while the lower values are associated with stable structures (Wołosiewicz, 2018). Wołosiewicz and Chybiorz (2015) suggested that drainage basin is considered tectonically active if K > 3, slightly active if the values of *K* are between 2 and 3, and tectonically inactive if K < 2. The K values are higher in all SW except for three SW (Giri Ganga, Paror, and Kharak ki Kiyar) (Table 2). The value of the K has been divided into Class-1 (> 6.11), Class-2 (4.59-6.10), Class-3 (3.06-4.58), and Class-4 (< 3.05) for GW based on tectonic activity (Table 3).

3.1.6 Ruggedness Number (R_n)

The Rn is the product of Dd and basin relief (Strahler, 1952). The Rn is the measure of the surface roughness or undulations which has direct correlation with geology, structure, and topography of the basin (Asthana et al., 2015). The Rn value ranges from 1.56 to 7.27, while the value of all other watersheds is listed in Table 2. The value of Rn has been divided based on influence of structure into Class-1 (> 5.85), Class-2 (4.41 – 5.84), Class-3 (2.98 – 4.40), and Class-4 (> 2.97) for GW (Table 3).

3.1.7 Asymmetry Factor (A_f)

The Asymmetry factor (A_f) reveals the tilt-block tectonics of the drainage basin (Cox, 1994; Keller and Pinter, 1996, Rawat et al., 2021). The A_f value also deciphers the possible directions of the differential tectonics or basin tilt (Pinter et al., 2006; Prakash et al., 2016). The A_f values equal to 50 suggests a symmetrical basin with no tectonic influence, while values more or less than 50 indicate an asymmetrical basin with possible tilting facilitated by local or regional tectonics and lithological variations (Sharma et al., 2018). The A_f values greater than 50 reveal left side tilting, while the A_f values less than 50 reveal right side tilting, in the direction of drainage (Molin et al., 2004; Prakash et al., 2016). The A_f value for 19 SW varies from 32.93 to 68.99 (Table 2). The value of A_f has been divided into Class-1 (> 68.1), Class-2 (60 – 68 and 31 – 37), Class-3 (37 – 42 and 57 - 60), and Class-4 (45 – 56) (Table 3).

3.1.8 Valley Floor Width to the Height Ratio (V_f)

The V_f is used to classify the river valleys into V-shaped, U-shaped, and flat valleys (Bull and McFadden, 1977; Keller and Pinter, 1996; Sharma et al, 2018). The deep V-shaped valley and long linear valley with active incision are generally associated with the active tectonic in the area; while U or flat-shaped valleys are indicators of less impact of tectonics; while flat valleys are associated with old stage of landform development, less activeness and base level attainment in the area (Keller, 1986; Keller and Pinter, 1996; Sharma et al, 2018). In Himalayan river basins, the valley is narrower in the headwaters due to a higher rate of tectonic activity and base level erosion which gradually gets lower towards the south showing wider valleys and river bank erosion (Bull and McFadden, 1977). The average V_f value for 19 SW ranges from 0.04 to 0.87 (Table 2). The V_f values

has been divided into the Class-1 (> 0.24), Class-2 (0.25 – 0.45), Class-3 (0.46 – 0.66), and Class-4 (> 0.67) for GW (Table 3).

3.1.9 Transverse Topography Symmetry Factor (*T*)

The *T* is also a symmetry parameter that interprets the lateral tilting or disturbances due to tectonic activities (Cox, 1994; Cox et al., 2001). The value of *T*=0 represents the symmetrical basin, while an increasing value of T or *T* > 0 is associated with an asymmetrical basin, the higher the value of *T* more will be the influence of tectonics on the basin (Cox, 1994; Keller and Pinter, 1996). The values *T* has been calculated for the different segments (Fig 3) in each sub-watershed and the values for 19 SW range from 0.01 to 0.81 (Table 2). The average T value ranges from 0.18 to 0.40 for 19 SW that has been divided into the Class-4 (> 0.21), Class-3 (0.22 – 0.41), Class-2 (0.42 – 0.61), and Class-1 (> 0.62) (Table 3).

3.1.10 Hypsometric Curve (HC) and Hypsometric Integral (*HI*)

The *hypsometric analysis* is an area-elevation analysis that is an important aspect to ascertain the erosional stage, degree of dissection, and influence of tectonics (Strahler, 1952; Horton, 1945; Ritter et al, 1995; Shukla et al, 2014). It is used to differentiate between the erosion of landforms at their different development stages i.e. youth, mature and old (Strahler, 1952; Horton, 1945; Ritter et al., 1995; Singh et al., 2008; Shukla et al., 2014; Yousaf et al., 2018). Strahler (1952) observed different types of hypsometric curves and categorized them for different stages of development of landforms. Hypsometric curves concave upwards with a low *HI* value suggests the old stage and lower rate of tectonic activity, whereas an S-shaped curve indicates the mature stage of landforms development with a moderate influence of tectonics, while a convex upwards curve with high *HI* value shows the youth stage of landforms development and high rate of tectonic activity in the basin (Strahler, 1952; Ritter et al., 1995; Keller and Pinter, 1996; Yousaf et al., 2018). The *HI* Value for 19 SW in GW ranges from 0.43 to 0.54 (Table 2). The HC for 19 SW for GW has shown a mature stage of development or S-shaped curve in most of the SW (Fig. 7). The *HI* values have been classified under Class-1 (> 0.51), Class-2 (0.48 – 0.50), Class-3 (0.45 – 0.47), and Class-4 < 0.45) for GW (Table 3).

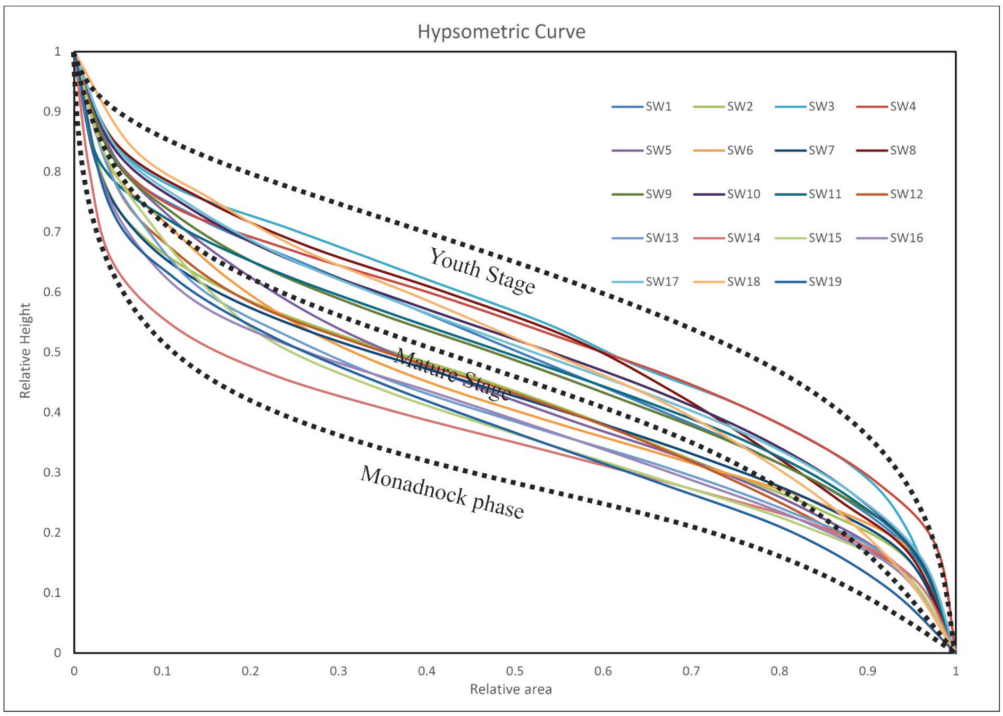

Figure 7 : Showing combined *Hypsometric Curve* (Vertical axes showing elative heights and horizontal axes as relative area) of SW of Giriwatershed, Himachal Pradesh, Northwest Himalaya.

3.2. Linear Aspects

3.2.1 Stream Length Gradient Index (S_L)

The SL is used in understanding the degree to which river systems have adapted to the region's landform evolution and tectonic activities. An S_L also accounts for the geological structure and climatic conditions, which may vary throughout the river's length. It is the relationship between the climatic variability and the *longitudinal profile* of the river to see the state of the equilibrium in the watershed or basin (Hack, 1973; Kotyari et al., 2017; Sharma et al, 2018). The S_L has been calculated along the main channel after being divided into segments (Fig 4; 5; 6) using natural break (Jenks) in the GIS environment.

The SL value for 19 SW ranges from 20 to 3572 (Fig 4; 5; 6), which has been divided into Class-1 (>2689), Class-2 (2688 - 1797), Class-3 (1796 - 909), and Class-4 (< 908) for GW based on the response of channel to climatic variability and active tectonics (Table 3).

3.2.2 Sinuosity Index (S_I)

The S_I is the ratio of the actual river path to the straight path of the river, which defines the degree of meandering. The S_I of a river is influenced by factors like geological structures, lithology, sediment load, etc. (Haggett and Chorley, 1969; Kothiyari et al., 2017; Das and Gupta, 2019). The S_I for the main channel of all 19 SW has been calculated by dividing the main channel into equal segments (Fig 4; 5; 6) based on natural break (Jenks) method in GIS. The SI value for 19 SW varies from 1.00 to 1.84 (Fig 4; 5; 6). Based on the results the SI values have been divided into Class-1 (>1.64), Class-2 (1.43 – 1.63), Class-3 (1.22 – 1.42), and Class-4 (< 1.21) suggesting the degree of tectonic control on main channel flow path (Table 3).

3.2.3 Longitudinal Profile Analysis

The *longitudinal profile* is a curve derived from the relationship between channel height and distance downstream, indicating the influence of gradient on the channel (Hack, 1973). *longitudinal profiles* have been obtained along main the channel as a plot between elevations and the distance of the river from head to mouth. The *longitudinal profile* helps in interpreting active tectonics, palaeo-climate, river discharge, sediment load, etc. (Hack, 1973; Leopold et al., 1964; Kothyari et al., 2017). In the GW, 15 SW have well-developed knick points along the main channel, indicating the influence of lithology and tectonics; while the remaining 4 SW have smoother profiles (Fig 4; 5; 6), indicating homogeneous lithology and minimal tectonic influence. The coefficient of determination (R^2) also has been calculated for the longitudinal profile of all river (Table 4), for linear, exponential, logarithmic, and power curves. The R2 is a crucial aspect for understanding the tectonic vulnerability of the basin, a higher value of R^2 is associated with highly active tectonic or vice-versa (Lee and Tsai, 2010).

Table 4 : Showing the Coefficient of Determination (R^2) for Longitudinal River Profile.

Subwatersheds	Coefficient of determination (R^2)			
	Linear	Exponential	Logarithmic	Power
SW1	0.9876	0.9972	0.5699	0.5219
SW2	0.9163	0.9603	0.6805	0.6093
SW3	0.964	0.9779	0.495	0.4165
SW4	0.9832	0.9731	0.5892	0.5123
SW5	0.7499	0.8151	0.7188	0.6733
SW6	0.8764	0.9278	0.5878	0.5878
SW7	0.734	0.8518	0.6494	0.74
SW8	0.9143	0.9727	0.5865	0.4984
SW9	0.8559	0.9284	0.6948	0.6177
SW10	0.9075	0.9553	0.6711	0.6043
SW11	0.9092	0.9584	0.5968	0.5228
SW12	0.8665	0.9497	0.6769	0.5645
SW13	0.8	0.9162	0.6919	0.5836
SW14	0.7771	0.9053	0.6557	0.5415
SW15	0.8149	0.9434	0.6664	0.5408
SW16	0.8262	0.9636	0.6894	0.5283
SW17	0.9031	0.9848	0.6674	0.525
SW18	0.9578	0.9979	0.6502	0.5232
SW19	0.9581	0.9909	0.5311	0.4263

3.2.4 Lineament and Drainage Interaction with Tectonics

The Himalayas are subjected to enormous stresses, which have resulted in the formation of numerous faults, *lineaments*, and shear zones, etc. (Singh et al., 2002; Yin, 2006). The lineaments are frequently interpreted as the visible surface of weak geologic

zones at tectonic boundaries, as well as faults and rock fractures (Thakur et al., 2007; Malik et al., 2010; Prakash et al., 2016). *Lineament* may be identified as the axis of the folds, a plane of the faults, long and narrow linear surface features, and linear tonal and textural contrast, etc. delineated from the satellite imageries, DEM, and Geological map (Parizek, 1976; Sander, 2007; Das and Gupta, 2019; Pant et al., 2020). *Lineaments* can be assessed to detect the role of the structure in shaping the topography or landforms in a river basin (Nur and Ban, 1982). The drainage channels passively follow faults or zones of weakness which is a common spatial relationship between rivers and geologic structures in the Himalayas (Sahoo et al., 2000). A total of 121 Major lineaments (Fig 2b; Fig 8) have been identified from satellite data. The majority of lineaments follow two directions predominantly, one is trending in the NE-SW and the second one is trending in the NW-SE (Fig. 8). The lower hemisphere equal-area net has been prepared for 3rd, 4th, and 5th order drainages which shows the majority of drainages flowing in N-S and E-W, N-S and E-W, S-W, and NW-SE directions respectively (Fig 9). The azimuth of drainages of the 3rd, 4th, and 5th have shown congruence with *lineament* azimuth suggesting structural control over the drainage channel (Fig 8).

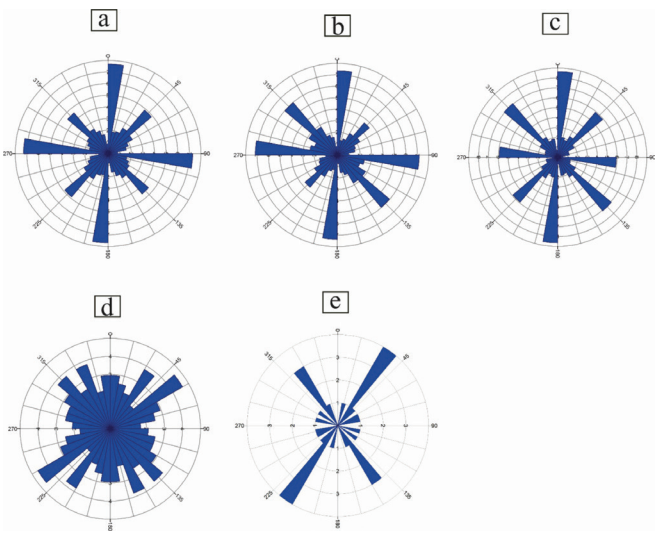

Figure 8 : Showing Rose diagram for Drainage (a, b, and c for 3rd, 4th, and 5th order drainage networks respectively), lineaments (d), and A_f parameter (e) for GW, Northwest Himalaya.

DISCUSSIONS

3.3 Spatial Aspects

The D_d gives an insight to spatial configuration and characteristics of the drainage network. The SW of Class-1 and Class-2 suggest the highly deformed and fragile nature of rocks in tectonically active terrain. The high D_d values are associated with rocks of incompetent nature, and are controlled by Krol, Khirkhi, Chaur, Jaunsar, Jutogh, and Giri thrusts (Fig 2a; Table 2) in GW. The higher Dd values are also supported by presence of knick points (Fig. 4; 5; 6), and high R^2 values in exponential curves for each sub-watershed (Table 4). The K and R_n reveal the gradient and undulation of the terrain (Chorley et al., 1957; Asthana et al., 2015). The SW classified in Class-1 and Class-2 suggest high K and R_n values inferring a higher incision rate, the presence of a narrow valley, and highly deformed terrain (Vijith and Satheesh, 2006). The results infer that the SW in Class-1 and Class-2 are influenced by the major structural discontinuity like Jaunsar, Giri, Jutogh, and Chaur thrusts (Fig 2a; Table 2).

The shape parameters viz. F_f, R_c, and B_s suggests that elongated basin shape and straight drainages are associated with high tectonic activity and structural control (Philip and Sah, 1999). The SW with lower F_f values (Class-1 and Class-2) are associated with active tectonics (Wołosiewicz, 2018) and are either lithologically or structurally controlled. The SW with lower Ff values in GW is possibly influenced by the Chaur, Jutogh, Jaunsar, and Giri thrusts (Fig 2a). The lower value of R_c is associated with tectonically active watersheds in comparison to the watersheds with a higher value. The SW with lower Rc values (Class-1 and Class-2) are associated with late youth to early mature stage of landform development, while watersheds with higher values are associated with mature to late mature stage of landform development that are also supported by HI values (Table 2). The SW with high B_s values suggests the region is tectonically active and is influenced by local and regional structures. The influence of regional structures on SW is also supported by availability of knick points in the *longitudinal profile* (Fig 4; 5; 6), F_f and R^2 values (Table 4). The results from shape parameters of 19 SW has suggested that majority of SW are elongated and their tributaries join the mainstream more or less at a right angle, suggesting significant role of tectonics in the SW (Fig 3).

The *HI* value deciphers the erosional and tectonic activity i.e. higher *HI* value shows

the development of the juvenile stage landforms and higher tectonic activities (El Hamdouni et al, 2008). The SW in Class-1 and Class-2 (Table 2; Fig 2a) are comparatively regions of high tectonic activities with highly deformed and lose rocks accompanied by major geological structure (Fig 2a). The *HI* values are also validated by the upward convex *HC* (Fig 7), exponential R2 value (Table 4), and the presence of knick points in *longitudinal profile* (Fig 4; 5; 6).

The A_f are crucial parameters that give insight to understand the possible tilting direction of the watershed or basin (Hare and Gardner, 1985; Cox, 1994; Keller and Pinter, 1996). The A_f values suggests that SW1, 3, 6, 7, 8, 9, 10, 11, 12, 13, 14, and SW19 are tilted towards left (i.e. in NE, and SW directions) of the main stream (Table 2). The Af values in these SW are influenced by geological structures like Krol, M.B.T., Giri, Jaunsar, Kullu, Jutogh, Khirkhi, and Chaur thrusts in these SW (Fig 4; 5; 6). While the Af value in SW2, 4, 5, 15, 16, 17, and SW18 show tilting on the right side (i.e. in NW and SE directions) of the main stream (Table 2) and are mainly influenced by M.B.T, Giri, Jutogh, and Chaur Thrusts (Fig 4; 5; 6). The major sub-watershed in the GW are showing tilting in the NE-SW direction which suggests, geological structure is controlling basin tilting and are still active (Fig 9).

The symmetry factor like *T* is also used for the assessment of the symmetry of the GW. The *T* show the possible tilt or symmetry in watershed or basin based upon the topographic symmetry along the main channel (Hare and Gardner, 1985; Keller and Pinter, 1996). The *T* values calculated for the 19 SW, which shows that all the SW are asymmetric in nature. The asymmetric behavior of all the SW in GW suggests that the watersheds are influenced by the ongoing tectonic processes. The SW with higher *T* suggests higher asymmetry and tilting of the basin due to active tectonics and higher rate of deformation (Cox, 1994) (Table 2), (Fig 2a). All SW show V_f values of less than one (Table 2) suggesting deep and narrow valleys and the significant influence of active tectonics (Table 2) (Sharma et al., 2018).

3.4 Linear Aspect

The values of the S_L from the results suggest that, it increase at places where the river flows over the structurally deformed or tectonically uplifted area (Keller and Pinter, 1996). The higher values of S_L in GW are associated with the segment of the river where

major thrust, local fault, and knick points encountered. In the GW, majority of SW show disequilibrium due to variable lithology and geological structure. In GW 18 SW has shown high exponential R^2 value except Paror watershed where it R^2 curve is linear suggesting very intense tectonic activity (Table 4).

The SI values from 19 SW suggest that in headwater regions or at higher elevations the main stream is flowing in more or less a straight path without any interference. The behavior of stream of flowing in straighter course suggests that the lithology in the region is homogenous with absence of geological structures or dormant tectonic activity, whereas the value of SI in the dispersing system or at lower elevation is comparatively higher which determines that there is heterogeneity in rock sequence and availability geological structure or active tectonics. The S_I value variation along the main stream is evidenced in the form of intense sinuosity and abrupt change in elevation (observed in the form of rapids) along the river course which clearly suggests the influence of tectonic and lithology over the drainage (Fig 4; 5; 6).

The azimuth of the 3rd, 4th, and 5th order drainage from 19 SW is drawn in lower hemisphere equal area stereonet which shows that the majority of streams has shown NE-SW and NW-SE trend. The 3rd drainage orders are used as they show the influence of geological structure and tectonics on drainage network development and arrangement. The trend of azimuths is correlated with lineament azimuths which shows that the trends from both parameters are consistent with each other suggesting geological structure and active tectonics is prevalent and crucial in the development of landforms.

3.5 Geomorphic Evidence of Neotectonics Activity

The geomorphic evidence of neotectonics activities like traces of fossil valley (Fig 9), Landslides, Denudational hills, Sag pond (Sirmouri Tal), triangular facets, displaced terraces, slope breaks, benches, and exceptionally wide and narrow valleys (Fig 10) are important active tectonic features in the GW (Philip and Sah, 1999; Kothyari et al., 2017; Thakur et al., 2021).

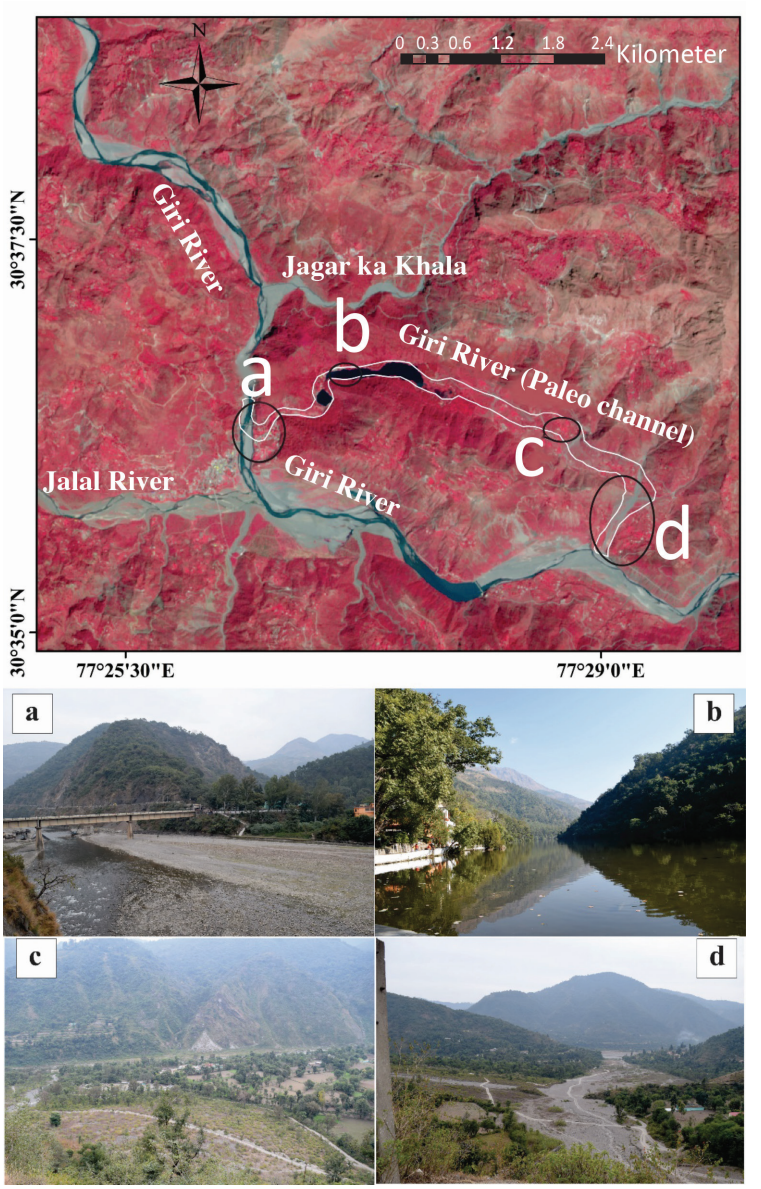

Figure 9 : Figure showing the different parts of the fossil valley including the Renuka Lake, near Renuka Ji area, Sirmour, Himachal Pradesh, northwest Himalaya, India.

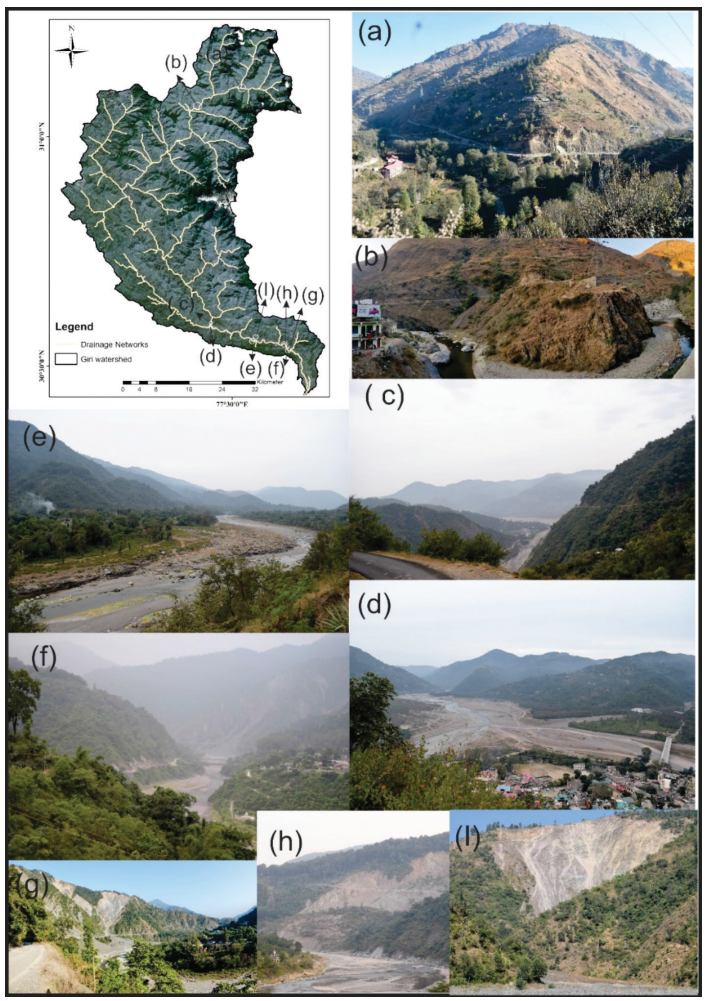

Figure 10 : Showing major consecutive wider and narrow segments in the mainstream, where (a) is a narrow valley and confluence of Giriganga and Chagunti Gad; (b) is meandering in upper segments of Giri river near, Chhailla, Gumma; (c) show upstream narrow segment; (d) show downstream very wide River segments near Dadhau; (e) show rock exposer in the River bed, and wide valley near Ambaun village; (f) show narrow downstream (g) show wide upstream River segments and major landslides near Sataun; (h) and (i) are major landslide near Sirmour Tal and Ambaun, Himachal Pradesh.

The fossil valleys are the results of the climate–tectonic interaction (Kothiyari and Juyal, 2013. The Giri River has changed its path in history which is observed with presence of about 7 km long fossil valley (Fig 9) (Rao, 1975; Raina, 1967). This event of changing of course can be attributed to a regional scale phenomenon aided by the upliftment and tilting (Rao, 1975). The main Giri river has deflected towards right (NE) about 1 km to 2.5 km from its current path after possible tilting of basin (Fig 9). The alteration in river valley profile (viz. narrow and wide valleys) in course of the Giri river (Fig 10) suggests significant role of the Giri thrust and MBT (Fig 2a; Fig 6) on the mainstream. Parenthetically, discontinuity developed by local and regional tectonic is attributing to formation of highly fragile, jointed, fractured, folded and faulted rock masses (Fig 11) in the GW, and making valley more susceptible in terms of disaster associated with active tectonics i.e. landslides, flooding, etc.

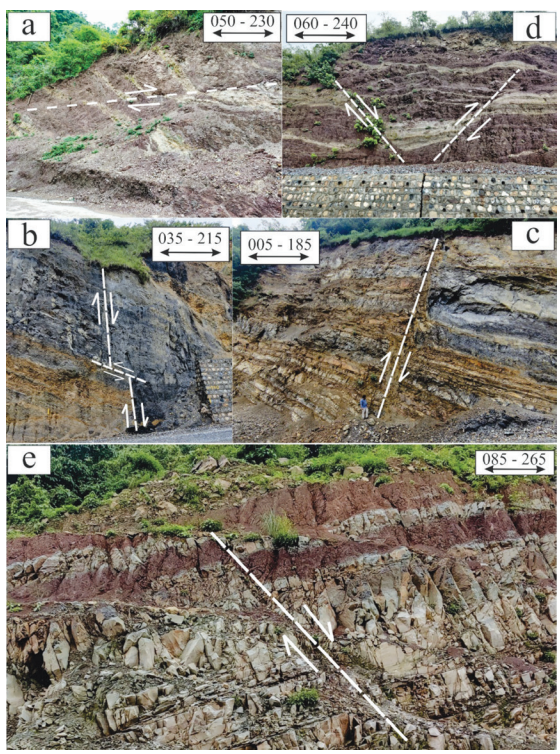

Figure 11 : Field photograph showing important faulted strata in the Giriwatershed, where (a), (c), and (c) are near Barwas, and (d) is near Kamrau village, and (e) is near Sirmouri Tal.

4. CONCLUSIONS

The GW is tectonically active and the activeness of the watershed is inferred by studying geomorphic indices for 19 SW, that are also convinced by the several geomorphic signatures in the GW. From the above study, the following assertion can be drawn:

- Geomorphic indices, river profile, drainages orientations, major lineaments, and field study suggests GW is tectonically active and is controlled by ongoing tectonic activities.
- The local and regional tectonics, lithological, and geomorphological factors play crucial role in shaping the landforms.
- The majority of SW suggested a NE-SW migration of litho-tectonic units in GW.
- Main Giri river around Renuka Ji have shifted around 1 – 2.5 km from its previous path, and have abandoned long stretch of paleo channel of about 7 km.
- The lower GW is tectonically more active in comparison to another part due to the complex geological structures and highly deformed rock mass, which is evidenced in the form of landslides, and other geomorphic signatures.
- Active tectonics activities are accelerating the rate of the geomorphic process like landslides, erosion, rock deformation, etc. in GW.

Acknowledgments

The author would like to thank University Grant Commission (UGC) for providing fellowship under the scheme of UGC JRF in terms of financial support. The authors are also thankful to the Department of Geology (HNB Garhwal University and DBS PG College, Dehradun), and the National Geotechnical facility for providing the necessary facility. The author also would like to thank Mr. Sandeep Jaglan (Research Scholar, Wadia Institute of Himalayan Geology, Dehradun) for his support. Last but not least authors are thankful to the anonymous reviewer for improving the manuscript.

References

1. Asthana, A.K.L., Gupta, A.K., Luirei, K., Bartarya, S.K., Rai, S.K. and Tiwari, S.K., 2015. A quantitative analysis of the Ramganga drainage basin and structural control on drainage pattern in the fault zones, Uttarakhand. Journal of the Geological Society of India, 86, pp.9-22.
2. Bhargava, O.N. and Srikantia, S.V., 2014. Geology and age of metamorphism of the Jutogh and Vaikrita Thrust Sheets, Himachal Himalaya. Himalayan Geology, 35(1), pp.1-15.
3. Biswas, M. and Paul, A., 2021. Application of geomorphic indices to Address the foreland Himalayan tectonics and landform deformation-Matiali-Chalsa-Baradighi recess, West Bengal, India. Quaternary International, 585, pp.3-14.
4. Biswas, M., Paul, A. and Jamal, M., 2021. Tectonics and channel morpho-hydrology—a quantitative discussion based on secondary data and field Investigation. Structural Geology and Tectonics Field Guidebook—Volume 1, pp.461-494. https://doi.org/10.1007/978-3-030-60143-0_16
5. Biyani, A.K., 2007. Dimensions of Himalayan geology. Satish Serial Publication. Azadpur, New Delhi, 330 p.
6. Bull, W.B. and McFadden, L.D., 1977. Tectonic geomorphology north and south of the Garlock fault, California. In Geomorphology in arid regions (pp. 115-138). Routledge.
7. Burke, K. and Dewey, J.F., 1973. Plume-generated triple junctions: key indicators in applying plate tectonics to old rocks. The Journal of Geology, 81(4), pp.406-433.
8. Chorley, R.J., Malm, D.E. and Pogorzelski, H.A., 1957. A new standard for estimating drainage basin shape. American journal of science, 255(2), pp.138-141.
9. Cox, R.T., 1994. Analysis of drainage-basin symmetry as a rapid technique to identify areas of possible Quaternary tilt-block tectonics: an example from the Mississippi Embayment. Geological society of america bulletin, 106(5), pp.571-581.
10. Cox, R.T., Van Arsdale, R.B. and Harris, J.B., 2001. Identification of possible Quaternary deformation in the northeastern Mississippi Embayment using quantitative geomorphic analysis of drainage-basin asymmetry. Geological Society of America Bulletin, 113(5), pp.615-624.
11. Das, S. and Gupta, K., 2019. Morphotectonic analysis of the Sali river basin, Bankura district, West Bengal. Arabian Journal of Geosciences, 12(7), p.244.
12. Dasgupta, S., Biswas, M., Mukherjee, S. and Chatterjee, R., 2022. Structural evolution and sediment depositional system along the transform margin-Palar–Pennar basin, Indian east coast. Journal of Petroleum Science and Engineering, 211, p.110155. https://doi.org/10.1016/j.petrol.2022.110155
13. DeMets, C., Gordon, R.G., Argus, D.F. and Stein, S., 1994. Effect of recent revisions to the geomagnetic reversal time scale on estimates of current plate motions. Geophysical research letters, 21(20), pp.2191-2194.
14. Dewey, J.F. and Bird, J.M., 1970. Mountain belts and the new global tectonics. Journal of geophysical Research, 75(14), pp.2625-2647.
15. Dhital, M.R., 2015. Geology of the Nepal Himalaya: regional perspective of the classic collided orogen. Springer. 498 p.
16. El Hamdouni, R., Irigaray, C., Fernández, T., Chacón, J. and Keller, E.A., 2008. Assessment of relative active tectonics, southwest border of the Sierra Nevada (southern Spain). Geomorphology, 96(1-2), pp.150-173.
17. Hack, J.T., 1973. Stream-profile analysis and stream-gradient index. Journal of Research of the us Geological Survey, 1(4), pp.421-429.
18. Haggett, P. and Chorley, R., 1969. Network Analysis in Geography (London). Edward Arnold.
19. Hare, P.W. and Gardner, T.W., 1985. Geomorphic indicators of vertical neotectonism along converging plate margins, Nicoya Peninsula, Costa Rica. Tectonic geomorphology, 4, pp.75-104.
20. Horton, R.E., 1945. Erosional development of streams and their drainage basins; hydrophysical approach to quantitative morphology. Geological society of America bulletin, 56(3), pp.275-370.
21. Hughes, N.C., Peng, S., Bhargava, O.N., Ahluwalia, A.D., Walia, S., Myrow, P.M. and Parcha, S.K., 2005. Cambrian biostratigraphy of the Tal Group, Lesser Himalaya, India, and early Tsanglangpuan (late early Cambrian) trilobites from the Nigali Dhar syncline. Geological Magazine, 142(1), pp.57-80.
22. Jain, A.K., Dasgupta, S.S., Bhargava, O.N., Israil, M., Patel, R.C., Mukul, M., Parcha, S.K., Adlakha, V., Agarwal, K.K., Singh, P. and Bhattacharyya, K., 2016. Tectonics and evolution of the Himalaya. Proceedings of the Indian national science academy.
23. Jamwal, C.S. and Wangu, A.K., 2012. Geology and mineral resources of Himachal Pradesh. Geological Survey of India, Miscellaneous Publication, 30(17), 1-49.
24. Jayangondaperumal, R., Mishra, R.L., Priyanka, R.S., Yadav, R.K., Mohanty, D.P., Pandey, A.R.J.U.N., Singh, I.S.H.W.A.R., Anil, A.R.A.V.I.N.D. and Dash, S.A.N.D.I.P.T.A., 2020, March. Active tectonics of Himalaya, Rift Basins in Central India and those related to crustal deformation at different time scales. In Proc Indian Natn Sci Acad (Vol. 86, No. 1, pp. 445-458).

25. Keller, E.A. and Pinter, N., 1996. Active tectonics (Vol. 338). Upper Saddle River, NJ: Prentice Hall. 338 p.
26. Keller, E.A., 1986. Investigation of active tectonics: use of surficial earth processes. Active tectonics, 1, pp.136-147.
27. Kothyari, G.C. and Juyal, N., 2013. Implications of fossil valleys and associated epigenetic gorges in parts of Central Himalaya. Current Science, pp.383-388.
28. Kothyari, G.C., Shukla, A.D. and Juyal, N., 2017. Reconstruction of Late Quaternary climate and seismicity using fluvial landforms in Pindar River valley, Central Himalaya, Uttarakhand, India. Quaternary International, 443, pp.248-264.
29. Lee, C.S. and Tsai, L.L., 2010. A quantitative analysis for geomorphic indices of longitudinal river profile: a case study of the Choushui River, Central Taiwan. Environmental Earth Sciences, 59, pp.1549-1558.
30. Leopold, L.B., Wolman, M.G. and Miller, J.P., 1964. Channel form and process. Fluvial processes in geomorphology. San Francisco, CA: WH Freeman and company, pp.198-322.
31. Lone, A., 2017. Morphometric and Morphotectonic Analysis of Ferozpur Drainage Basin Left Bank Tributary of River Jhelum of Kashmir Valley, NW Himalayas, India. J. Geogr. Nat. Disasters, 7(1000208), pp.1-1000208. Doi: 10.4172/2167-0587.1000208
32. Mahmood, S.A. and Gloaguen, R., 2012. Appraisal of active tectonics in Hindu Kush: Insights from DEM derived geomorphic indices and drainage analysis. Geoscience Frontiers, 3(4), pp.407-428.
33. Mesa, L.M., 2006. Morphometric analysis of a subtropical Andean basin (Tucuman, Argentina). Environmental Geology, 50(8), pp.1235-1242.
34. Miller, V.C., 1953. A quantitative geomorphic study of drainage basin characteristics in the clinch mountain area Virginia and Tennessee. Columbia Univ New York. Technical Report 3, Office of the Naval Research, Department of Geology, Columbia University, New York.
35. Mishra, P. and Mukhopadhyay, D.K., 2012. Structural evolution of the frontal fold–thrust belt, NW Himalayas from sequential restoration of balanced cross-sections and its hydrocarbon potential. Geological Society, London, Special Publications, 366(1), pp.201-228.
36. Molin, P., Pazzaglia, F.J. and Dramis, F., 2004. Geomorphic expression of active tectonics in a rapidly-deforming forearc, Sila massif, Calabria, southern Italy. American journal of science, 304(7), pp.559-589.
37. Mukherjee, S., 2015. A review on out-of-sequence deformation in the Himalaya. Special Publications, 412(1), pp.67-109.
38. Mukhopadhyay, D.K., Bhadra, B.K., Ghosh, T.K. and Srivastava, D.C., 1996. Evidence for the thrust emplacement of the 'Lesser Himalaya'Chur granite, Himachal Pradesh. Proceedings of the Indian Academy of Sciences-Earth and Planetary Sciences, 105, pp.157-171.
39. Nakata, T., 1972. Geomorphic history and crustal movements of the foothills of the Himalayas. Science Reports of the Tohoku University, 7th Series (Geography), 22, pp.39-177.
40. Negi, R., Sati, S.P., Kumar, D. and Rana, S.S., 2021. Assessment of Landslides Susceptibility in Giri Watershed, Northwest Himalaya, Himachal Pradesh, India. Journal of Mountain Research, 16 (1), 45–59. https://doi.org/10.51220/jmr.v16i1.5
41. Nur, A. and Ben Avraham, Z., 1982. Oceanic plateaus, the fragmentation of continents, and mountain building. Journal of Geophysical Research: Solid Earth, 87(B5), pp.3644-3661.
42. Ozdemir, H. and Bird, D., 2009. Evaluation of morphometric parameters of drainage networks derived from topographic maps and DEM in point of floods. Environmental geology, 56, pp.1405-1415.
43. Parizek, R.R., 1976. On the nature and significance of fracture traces and lineaments in carbonate and other terranes. V. (Ed.), Karst Hydrology and Water Resources. Water Resources Publications, Fort Collins, CO, 47 – 108.
44. Pérez-Peña, J.V., Azañón, J.M. and Azor, A., 2009. CalHypso: An ArcGIS extension to calculate hypsometric curves and their statistical moments. Applications to drainage basin analysis in SE Spain. Computers & Geosciences, 35(6), pp.1214-1223.
45. Philip, G. and Sah, M.P., 1999. Geomorphic signatures of active tectonics in the Trans-Yamuna segment of the western Doon valley, northwest Himalaya, India. International journal of applied earth observation and geoinformation, 1(1), pp.54-63.
46. Pike, R.J. and Wilson, S.E., 1971. Elevation-relief ratio, hypsometric integral, and geomorphic area-altitude analysis. Geological Society of America Bulletin, 82(4), pp.1079-1084.
47. Pinter, N., Grenerczy, G., Weber, J., Medak, D. and Stein, S. eds., 2006. The Adria microplate: GPS geodesy, tectonics and hazards (Vol. 61). Springer Science & Business Media.
48. Prakash, K., Mohanty, T., Singh, S., Chaubey, K. and Prakash, P., 2016. Drainage morphometry of the Dhasan river basin, Bundelkhand craton, central India using remote sensing and GIS techniques. Journal of Geomatics, 10(2), pp.122-132.
49. Puniya, M.K., Patel, R.C. and Pant, P.D., 2019. Structural and thermochronological studies of the Almora klippe, Kumaun, NW India: implications for crustal thickening and exhumation of the NW Himalaya. Geological Society, London, Special Publications, 481(1), pp.81-110.

50. Raina, B.N., 1967. A note on the origin of some Himalayan Lakes. Proceedings of Seminar on Geomorphological studies in India, University of Sauger, 101–113.
51. Ramírez Herrera, M.T., 1998. Geomorphic assessment of active tectonics in the Acambay Graben, Mexican volcanic belt. Earth Surface Processes and Landforms: The Journal of the British Geomorphological Group, 23(4), pp.317-332.
52. Rao D., 1975. On the origin of Renuka lake. Journal of the Indian Society of Photo-Interpretation, 3, pp.37-41.
53. Rawat, A., Banerjee, S. and Sundriyal, Y., 2021. Geomorphological and Statistical Assessment of Tilt-Block Tectonics in the Garhwal Synform: Implications for the Active Tectonics, Garhwal Lesser Himalaya, India. Geosciences, 11(8), p.345.
54. Ritter, D.F., Kochel, R.C., Miller, J.R. and Miller, J.R., 1995. Process geomorphology (No. 551.4 R5). Dubuque, Iowa: Wm. C. Brown.
55. Sah, N., Kumar, M., Upadhyay, R. and Dutt, S., 2018. Hill slope instability of Nainital City, Kumaun Lesser Himalaya, Uttarakhand, India. Journal of rock mechanics and geotechnical engineering, 10(2), pp.280-289.
56. Sahoo, P.K., Kumar, S. and Singh, R.P., 2000. Neotectonic study of Ganga and Yamuna tear faults, NW Himalaya, using remote sensing and GIS. International Journal of Remote Sensing, 21(3), pp.499-518.
57. Sander, P., 2007. Lineaments in groundwater exploration: a review of applications and limitations. Hydrogeology journal, 15(1), pp.71-74.
58. Sati, S.P., Rana, N., Kumar, D., Reddy, D.V. and Sundriyal, Y.P., 2008. Pull-apart origin of wider segments of the Alaknanda Basin Uttarakhand Himalaya, India. Himalayan Geology, 29(3), pp.89-91.
59. Sharma, G., Champati ray PK, and Mohanty S (2018). Morphotectonic analysis and GNSS observations for assessment of relative tectonic activity in Alaknanda basin of Garhwal Himalaya, India. Geomorphology, 301, pp.108-120.
60. Shukla, D.P., Dubey, C.S., Ningreichon, A.S., Singh, R.P., Mishra, B.K. and Singh, S.K., 2014. GIS-based morpho-tectonic studies of Alaknanda river basin: a precursor for hazard zonation. Natural hazards, 71, pp.1433-1452.
61. Singh, B.P., Bhargava, O.N., Mikuláš, R., Morrision, S., Kaur, R., Singla, G., Kishore, N., Kumar, N., Kumar, R. and Moudgil, S., 2020. Integrated sedimentological, ichnological and sequence stratigraphical studies of the Koti Dhaman Formation (Tal Group), Nigali Dhar Syncline, Lesser Himalaya, India: paleoenvironmental, paleoecological, paleogeographic significance. Ichnos, 27(1), pp.1-34.
62. Singh, C.P., 2002. Applied geomorphology: a study. BR Publishing Corporation, Delhi.
63. Singh, O., Sarangi, A. and Sharma, M.C., 2008. Hypsometric integral estimation methods and its relevance on erosion status of north-western lesser Himalayan watersheds. Water Resources Management, 22, pp.1545-1560.
64. Singh, S.K., Mohanty, W.K., Bansal, B.K. and Roonwal, G.S., 2002. Ground motion in Delhi from future large/great earthquakes in the central seismic gap of the Himalayan arc. Bulletin of the Seismological Society of America, 92(2), pp.555-569.
65. Srikantia, S.V. and Bhargava, O.N., 2021. Geology of Himachal Pradesh. GSI Publications, 2(1).
66. Strahler, A.N., 1952. Hypsometric (area-altitude) analysis of erosional topography. Geological society of America bulletin, 63(11), pp.1117-1142.
67. Strahler, A.N., 1964. Quantitative geomorphology of drainage basin and channel networks. Handbook of applied hydrology.
68. Thakur, M., Kumar, N. and Dhiman, R.K., 2021, December. Geological Investigation of Sataun Landslide along the Trans-Yamuna Active Fault System, Northwestern Himalaya, India. In AGU Fall Meeting Abstracts (Vol. 2021, pp. NH35E-0510).
69. Vijith, H. and Satheesh, R., 2006. GIS based morphometric analysis of two major upland sub-watersheds of Meenachil river in Kerala. Journal of the Indian Society of Remote Sensing, 34, pp.181-185.
70. Vijith, H., Seling, L.W. and Dodge-Wan, D., 2018. Estimation of soil loss and identification of erosion risk zones in a forested region in Sarawak, Malaysia, Northern Borneo. Environment, development and sustainability, 20(3), pp.1365-1384.
71. Webb, A.A.G., Yin, A., Harrison, T.M., Célérier, J. and Burgess, W.P., 2007. The leading edge of the Greater Himalayan Crystalline complex revealed in the NW Indian Himalaya: Implications for the evolution of the Himalayan orogen. Geology, 35(10), pp.955-958.
72. Webb, A.A.G., Yin, A., Harrison, T.M., Célérier, J., Gehrels, G.E., Manning, C.E. and Grove, M., 2011. Cenozoic tectonic history of the Himachal Himalaya (northwestern India) and its constraints on the formation mechanism of the Himalayan orogen. Geosphere, 7(4), pp.1013-1061.
73. Wołosiewicz, B. & Chybiorz, R., 2015. Application of the morphometric and remote sensing methods for studies on neotectonic activity of Pieniny Seismic Region. In: Conference materials: IV Conference GIS in science, Poznań 2015.
74. Wołosiewicz, B., 2016. Morphotectonic control of the Białka drainage basin (Central Carpathians): Insights from DEM and morphometric analysis.

75. Wołosiewicz, B., 2018. The influence of the deep seated geological structures on the landscape morphology of the Dunajec River catchment area, Central Carpathians, Poland and Slovakia. Contemporary Trends in Geoscience, 7.
76. Yin, A., 2006. Cenozoic tectonic evolution of the Himalayan orogen as constrained by along-strike variation of structural geometry, exhumation history, and foreland sedimentation. Earth-Science Reviews, 76(1-2), pp.1-131.
77. Yousaf, W., Mohayud-Din-Hashmi, S.G., Akram, U., Saeed, U., Ahmad, S.R., Umar, M. and Mubashir, A., 2018. Erosion potential assessment of watersheds through GIS-based hypsometric analysis: a case study of Kurram Tangi Dam. Arabian Journal of Geosciences, 11, pp.1-9.
78. Kothyari, G.C., Joshi, N., Taloor, A.K., Kandregula, R.S., Kotlia, B.S., Pant, C.C. and Singh, R.K., 2019. Landscape evolution and deduction of surface deformation in the Soan Dun, NW Himalaya, India. Quaternary International, 507, pp.302-323.
79. Kothyari, G.C., Kotlia, B.S., Talukdar, R., Pant, C.C. and Joshi, M., 2020. Evidences of neotectonic activity along Goriganga river, higher central Kumaun Himalaya, India. Geological Journal, 55(9), pp.6123-6146.
80. Thakur, M., Kumar, N., Dhiman, R.K. and Malik, J.N., 2023. Geological and geotechnical investigations of the Sataun landslide along the Active Sirmauri Tal Fault, Sataun, Northwestern Himalaya, India. Landslides, 20(5), pp.1045-1063.
81. Pant, N., Dubey, R.K., Bhatt, A., Rai, S.P., Semwal, P. and Mishra, S., 2020. Soil erosion and flood hazard zonation using morphometric and morphotectonic parameters in Upper Alaknanda river basin. Natural Hazards, 103, pp.3263-3301.
82. Gautam, P.K., Gahalaut, V.K., Prajapati, S.K., Kumar, N., Yadav, R.K., Rana, N. and Dabral, C.P., 2017. Continuous GPS measurements of crustal deformation in Garhwal-Kumaun Himalaya. Quaternary International, 462, pp.124-129.
83. Yadav, R.K., Gahalaut, V.K., Bansal, A.K., Sati, S.P., Catherine, J., Gautam, P., Kumar, K. and Rana, N., 2019. Strong seismic coupling underneath Garhwal–Kumaun region, NW Himalaya, India. Earth and Planetary Science Letters, 506, pp.8-14.
84. Thakur, V.C., Pandey, A.K. and Suresh, N., 2007. Late Quaternary–Holocene evolution of dun structure and the Himalayan Frontal fault zone of the Garhwal sub-Himalaya, NW India. Journal of Asian Earth Sciences, 29(2-3), pp.305-319.
85. Mueller, J.E., 1968. An introduction to the hydraulic and topographic sinuosity indexes. Annals of the association of american geographers, 58(2), pp.371-385.
86. Malik, J.N., Shah, A.A., Sahoo, A.K., Puhan, B., Banerjee, C., Shinde, D.P., Juyal, N., Singhvi, A.K. and Rath, S.K., 2010. Active fault, fault growth and segment linkage along the Janauri anticline (frontal foreland fold), NW Himalaya, India. Tectonophysics, 483(3-4), pp.327-343.